

# Numerical solution of non-Newtonian nanofluid flow over a stretching sheet

S. Nadeem · Rizwan Ul Haq · Z. H. Khan

Received: 27 April 2013 / Accepted: 13 May 2013 / Published online: 5 June 2013  
© The Author(s) 2013. This article is published with open access at Springerlink.com

**Abstract** The steady flow of a Jeffrey fluid model in the presence of nano particles is studied. Similarity transformation is used to convert the governing partial differential equations to a set of coupled nonlinear ordinary differential equations which are solved numerically. Behavior of emerging parameters is presented graphically and discussed for velocity, temperature and nanoparticles fraction. Variation of the reduced Nusselt and Sherwood number against physical parameters is presented graphically. It was found that reduced Nusselt number is decreasing function and reduced Sherwood number is increasing function of Brownian parameter  $N_b$  and thermophoresis parameter  $N_t$ .

**Keywords** Jeffrey fluid model · Nanofluid flow · Stretching sheet · Brownian motion · Thermophoresis · Numerical solution

## Introduction

Study of non-Newtonian fluids over a stretching surface achieved great attention due to its large number of application. Infact, the effects of non-Newtonian behavior can be determined due to its elasticity, but sometimes rheological properties of fluid are identified by their constitutive equations. In view of rheological parameters, the constitutive equations in the non-Newtonian fluids are more

complex and thus give rise the equations which are complicated than the Navier–Stokes equations. Many of the fluids used in the oil industry and simulate reservoirs are significantly non-Newtonian. In different degree, they display shear-dependent of viscosity, thixotropy and elasticity (Pearson and Tardy 2002; Ellahi and Afza 2009; Ellahi 2009).

The study of two-dimensional flow over a linear stretching surface achieved great interest due to its particle application in engineering and industrial area for expanding and contracting of surfaces such as stretching/shrinking wrapping, bundle wrapping, hot rolling, extrusion of sheet material, wire rolling, glass fiber, metal packaging and aluminum bottle manufacturing processes, etc. Initially, Crane (1970) presents the concept of stretching sheet and obtained the closed form solution for the flow of viscous fluid over a stretching surface. Concept of boundary layer flow over a moving surface is presented by Sakiadis (1961). Later on many authors extended the idea of stretching sheet for different fluid models (Nadeem and Hussain 2010; Nadeem et al. 2011, 2012; Noor et al. 2010; Hashim et al. 2008).

Recently, nanofluids have achieved admirable attention due to its practical applications. Nanofluids are actually homogenous mixture of base fluid and nanoparticles. The concept of nanofluids refers to a new kind of heat transport fluids by suspending nano-scaled metallic and nonmetallic particles in base fluids. Few examples of common base fluids are water, organic liquids (e.g. ethylene, tri-ethylene-glycols, refrigerants, etc.), oil and lubricants, bio-fluids, polymeric solution and other common liquids. Initially, the name of nanofluid was presented by Choi (1995), in which he described the suspension containing ultra-fine particles (diameter less than 50 nm). Xuan et al. (2003) applied the theory of Brownian motion and diffusion-limited

S. Nadeem · R. U. Haq (✉)  
Department of Mathematics, Quaid-I-Azam University 45320,  
Islamabad 44000, Pakistan  
e-mail: ideal\_riz@hotmail.com; snqau@hotmail.com

Z. H. Khan  
School of Mathematical Sciences, Peking University,  
Beijing 100871, People's Republic of China

aggregation model to simulate random motion and the aggregation process of the nanoparticles. Nanofluid for heat transfer along with the thermal conductivity for various materials was discussed by Cheng (2009). Initially, Khan and Pop (2010) discussed the effects of nanoparticles for stretching sheet. In his article, he described the laminar fluid flow over a stretching sheet in a nanofluid. After this, Khan and Aziz (2011) perform for natural convection flow of a nanofluid over a vertical plate with uniform surface heat flux. Similarity reductions for problems of magnetic field effects on free convection flow of a nanofluid past a semi-infinite vertical flat plate has been discussed by Hamad et al. (2011). Large numbers of investigation have also taken related to the exponentially stretching sheet for

nanofluids. Initially, Nadeem and Lee (2012) discussed the boundary layer flow of nanofluid over an exponentially stretching surface. Later on many investigations related to the nanofluids for various fluid models are presented (Sebdani et al. 2012; Ma 2012).

In this paper, our main objective is to investigate Jeffrey fluid model for nanofluid over a stretching sheet. Only few articles related to the nanofluid for non-Newtonian models are considered (Domairry et al. 2012). The governing systems of partial equations have been transformed to set of coupled ordinary differential equations with the help of suitable similarity transformations and boundary layer approach. The reduced equations are solved numerically. The pertinent parameters of nano non-Newtonian fluid are discussed

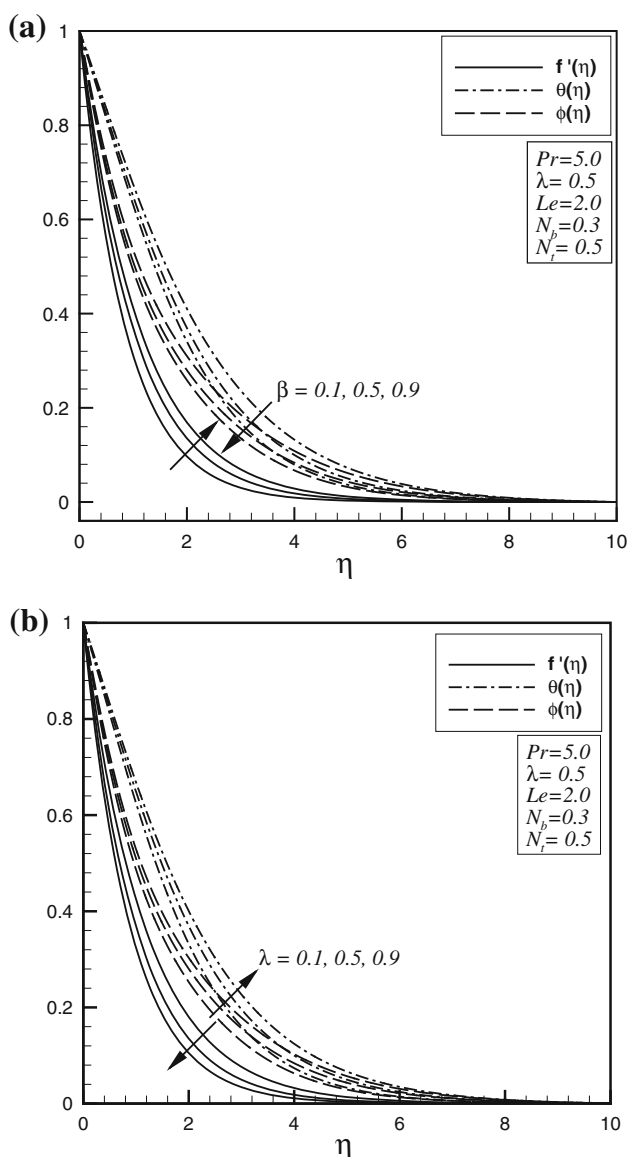


**Fig. 1** Effects of  $\beta$  and  $\lambda$  on velocity profile  $f'(\eta)$ , temperature profile  $\theta(\eta)$  and nanoparticle fraction  $\phi(\eta)$ , respectively

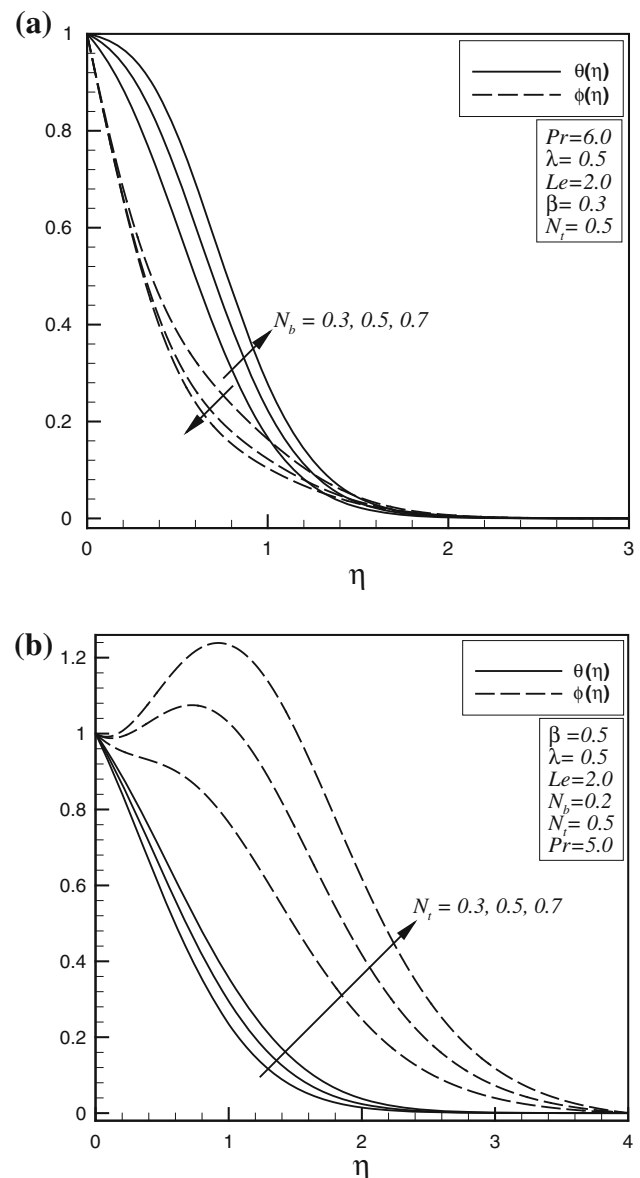


**Fig. 2** Effects of  $N_b$  and  $N_t$  on temperature profile  $\theta(\eta)$  and nanoparticle fraction  $\phi(\eta)$ , respectively

through graphs and compare it with table. The expression for local Nusselt number and local Sherwood number also counted numerically and discussed through graphs.

### Problem formulation

Consider two-dimensional steady incompressible fluid past a stretching sheet. In addition, nanoparticles effects are saturated, while sheet is stretching with the plane  $y = 0$ . The flow is assumed to be confined to  $y > 0$ . In the present case, we assumed that sheet is stretched with the linear velocity  $u_w(x) = ax$ , where  $a > 0$  is constant and  $x$  axis is measured along the stretching surface. The boundary layer equations of Jeffrey fluid along nanoparticles are given as follows:

$$\frac{\partial u}{\partial x} + \frac{\partial v}{\partial y} = 0, \quad (1)$$

$$u \frac{\partial u}{\partial x} + v \frac{\partial u}{\partial y} = \frac{\nu}{1 + \lambda} \left[ \frac{\partial^2 u}{\partial y^2} + \lambda_1 \left( u \frac{\partial^3 u}{\partial x \partial y^2} - \frac{\partial u}{\partial x} \frac{\partial^2 u}{\partial y^2} + \frac{\partial u}{\partial y} \frac{\partial^2 u}{\partial x \partial y} + v \frac{\partial^3 u}{\partial y^3} \right) \right], \quad (2)$$

$$u \frac{\partial T}{\partial x} + v \frac{\partial T}{\partial y} = \alpha \left( \frac{\partial^2 T}{\partial x^2} + \frac{\partial^2 T}{\partial y^2} \right) + \tau \left\{ D_B \left( \frac{\partial C}{\partial x} \frac{\partial T}{\partial x} + \frac{\partial C}{\partial y} \frac{\partial T}{\partial y} \right) + \left( \frac{D_T}{T_\infty} \right) \left[ \left( \frac{\partial T}{\partial x} \right)^2 + \left( \frac{\partial T}{\partial y} \right)^2 \right] \right\}, \quad (3)$$

$$u \frac{\partial C}{\partial x} + v \frac{\partial C}{\partial y} = D_B \left( \frac{\partial^2 C}{\partial x^2} + \frac{\partial^2 C}{\partial y^2} \right) + \left( \frac{D_T}{T_\infty} \right) \left( \frac{\partial^2 T}{\partial x^2} + \frac{\partial^2 T}{\partial y^2} \right), \quad (4)$$

where  $u$  and  $v$  denote the respective velocities in the  $x$  and  $y$  directions, respectively,  $\rho_f$  is the density of the base fluid,  $\nu$  is the kinematic viscosity of the fluid,  $\sigma$  is the electrical conductivity,  $\rho$  being the density of the fluid,  $\lambda$  and  $\lambda_1$  are ratio of relaxation to retardation times and retardation time, respectively,  $\alpha$  is the thermal diffusivity,  $T$  the fluid temperature,  $C$  the nanoparticles fraction,  $T_w$  and  $C_w$  are the temperature of fluid and nanoparticles fraction at wall, respectively,  $D_B$  the Brownian diffusion coefficient,  $D_T$  is the thermophoretic diffusion coefficient,  $\tau = \frac{(\rho c)_p}{(\rho c)_f}$  is the ratio between the effective heat capacity of the nanoparticles material and heat capacity of the fluid,  $C$  is the volumetric volume expansion coefficient,  $\rho_p$  is the density of the particles, when  $y$  tends to infinity then the ambient values of  $T$  and  $C$  are denoted by  $T_\infty$  and  $C_\infty$ . The associated boundary conditions of Eqs. (2)–(4) are as follows:

$$\begin{aligned} u &= u_w(x) = ax, \quad v = 0, \quad T = T_w, \quad C = C_w \quad \text{at } y = 0, \\ u &= 0, \quad v = 0, \quad u_y = 0, \quad T = T_\infty, \quad C = C_\infty \quad \text{as } y \rightarrow \infty. \end{aligned} \quad (5)$$

Introducing the following similarity transformations,

$$\begin{aligned} \psi &= (av)^{1/2} x f(\eta), \quad \theta(\eta) = \frac{T - T_\infty}{T_w - T_\infty} \\ \varphi(\eta) &= \frac{C - C_\infty}{C_w - C_\infty}, \quad \eta = \sqrt{\frac{a}{\nu}} y, \end{aligned} \quad (6)$$

where the stream function  $\psi$  is defined as  $u = \frac{\partial \psi}{\partial y}$  and  $v = -\frac{\partial \psi}{\partial x}$ . Making use of Eq. (6), equation of continuity is identically satisfied and Eqs. (2)–(4) along with (5) take the following form:

$$f''' + \beta(f''^2 - ff''''') + (1 + \lambda)(ff'' - f'^2) = 0, \quad (7)$$

$$\theta'' + \text{Pr}[f\theta' + N_b(\theta'\varphi') + N_t(\theta')^2] = 0, \quad (8)$$

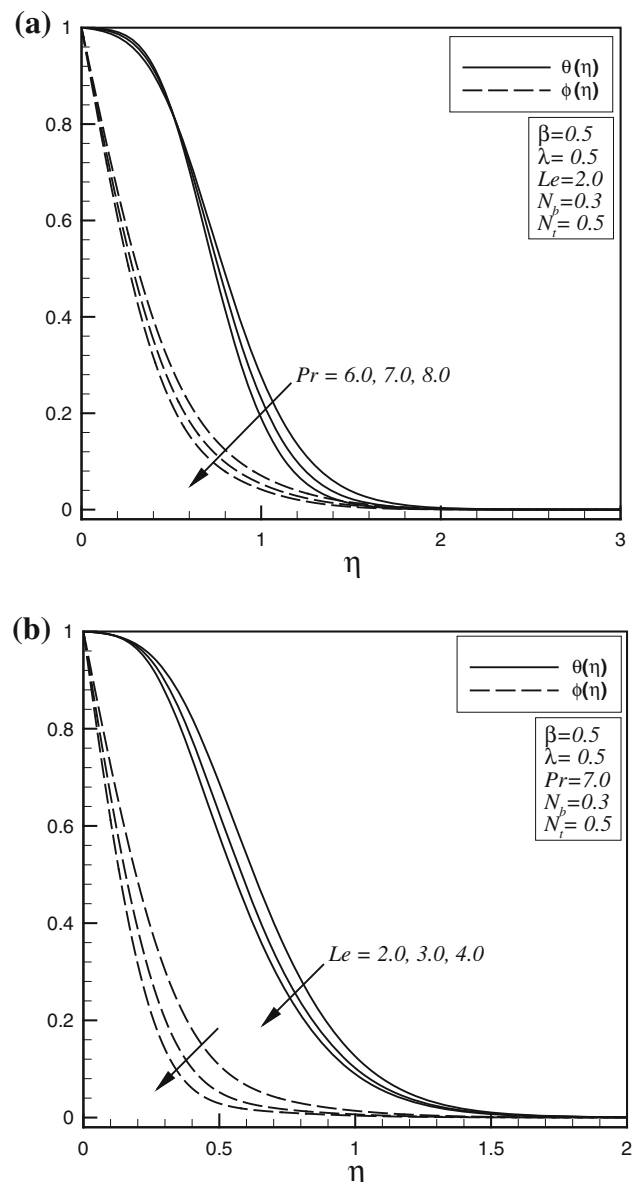


**Fig. 3** Effects of  $Pr$  and  $Le$  on temperature profile  $\theta(\eta)$  and nanoparticle fraction  $\varphi(\eta)$ , respectively

**Table 1** Comparison of numerical values for local Nusselt number  $Re_x^{-1/2}Nu_x$  in the absence of non-Newtonian effects, i.e., ( $\beta = \lambda = 0$ ) when  $Pr = 10$  and  $Le = 1$

	$N_b = 0.1$		$N_b = 0.3$		$N_b = 0.5$	
	Khan (2010)	Present study	Khan (2010)	Present study	Khan (2010)	Present study
$N_t \downarrow$	$-\theta'(0) \downarrow$	$-\theta'(0) \downarrow$	$-\theta'(0) \downarrow$	$-\theta'(0) \downarrow$	$-\theta'(0) \downarrow$	$-\theta'(0) \downarrow$
0.1	0.9524	0.95247	0.2522	0.25223	0.0543	0.05433
0.3	0.5201	0.52013	0.1255	0.13554	0.0291	0.02918
0.5	0.311	0.32110	0.0833	0.08336	0.0179	0.01794

**Table 2** Comparison of numerical values for local Sherwood number  $Re_x^{-1/2}Sh$  in the absence of non-Newtonian effects, i.e., ( $\beta = \lambda = 0$ ) when  $Pr = 10$  and  $Le = 1$

	$N_b = 0.1$		$N_b = 0.3$		$N_b = 0.5$	
	Khan (2010)	Present study	Khan (2010)	Present study	Khan (2010)	Present study
$N_t \downarrow$	$-\phi'(0) \downarrow$	$-\phi'(0) \downarrow$	$-\phi'(0) \downarrow$	$-\phi'(0) \downarrow$	$-\phi'(0) \downarrow$	$\phi'(0) \downarrow$
0.1	2.1294	2.12946	2.4100	2.41002	2.3836	2.38362
0.3	2.5286	2.52861	2.6088	2.60881	2.4984	2.49847
0.5	3.0351	3.03515	2.7519	2.75199	2.5731	2.57313

**Table 3** Comparison of numerical values for local Nusselt number  $Re_x^{-1/2}Nu_x$  and the local Sherwood number  $Re_x^{-1/2}Sh$  in the presence of the effects of non-Newtonian fluid when  $\lambda = 0.5$ ,  $\beta = 0.5$ ,  $Pr = 10$  and  $Le = 1$

$N_b \downarrow$	$N_t = 0.1$		$N_t = 0.3$		$N_t = 0.5$	
	$-\theta'(0) \downarrow$	$-\phi'(0) \downarrow$	$-\theta'(0) \downarrow$	$-\phi'(0) \downarrow$	$-\theta'(0) \downarrow$	$-\phi'(0) \downarrow$
0.1	1.710019	-0.763686	1.302975	-2.308676	0.990168	-2.798262
0.3	1.144226	0.311453	0.845832	0.042291	0.628085	0.003197
0.5	0.708856	0.499848	0.509359	0.439533	0.370789	0.458568
0.7	0.402155	0.562068	0.282112	0.563054	0.202194	0.591438

$$\varphi'' + Le Pr(f\varphi') + \frac{N_t}{N_b}\theta'' = 0, \quad (9)$$

$$f(0) = 0, f'(0) = 1, f'(\infty) = 0, f''(\infty) = 0 \quad (10)$$

$$\theta(0) = 1, \theta(\infty) = 0, \quad (11)$$

$$\varphi(0) = 1, \varphi(\infty) = 0. \quad (12)$$

In these expressions  $\beta = \lambda_1 c$  is Deborah number,  $Pr = \frac{\nu}{\alpha}$  is Prandtl number,  $N_b = \frac{(\rho c)_p D_B (\varphi_w - \varphi_\infty)}{\nu(\rho c)_p}$  represents the Brownian motion,  $N_t = \frac{(\rho c)_p D_T (T_w - T_\infty)}{\nu(\rho c)_p}$  thermophoresis parameter,  $Le = \frac{\alpha}{D_B}$  the Lewis number. Expressions for the local Nusselt number  $Nu$  and the local Sherwood number  $Sh$  are defined as,

$$Nu = \frac{xq_w}{\alpha(T_w - T_\infty)}, \quad Sh = \frac{xq_m}{D_B(C_w - C_\infty)}, \quad (13)$$

where  $q_w$  and  $q_m$  are the heat flux and mass flux, respectively.

$$q_w = -\alpha \left( \frac{\partial T}{\partial y} \right)_{y=0}, \quad q_m = -D_B \left( \frac{\partial C}{\partial y} \right)_{y=0}. \quad (14)$$

Dimensionless form of Eq. (13) takes the form

$$Re_x^{-1/2}Nu = -\theta'(0), \quad Re_x^{-1/2}Sh = -\phi'(0), \quad (15)$$

where  $Re_x = u_w(x)x/\nu$  is local Reynolds number based on the stretching velocity  $u_w(x)$ .

## Numerical technique

The system of coupled non-linear coupled differential equations (7)–(9) along with the boundary conditions (10) and (12) is solved numerically using fourth-order Runge–Kutta–Fehlberg method with a shooting technique. The step size  $\Delta\eta = 0.001$  is used to obtain the numerical solution with  $\eta_{\max}$ , and accuracy to the fifth decimal place as the criterion of convergence. The boundary value problem function,

$$y' = f(x, y), \quad a \leq x \leq b, \quad (16)$$

is subject to the two-point boundary value problem:

$$bc(y(a), y(b)) = 0. \quad (17)$$

The approximate solution  $S(x)$  is a continuous function that is cubic polynomial on each subinterval  $[x_n, \dots, x_{n+1}]$  of the mesh  $a = x_0 < x_1 < x_2 < \dots < x_N = b$ . It satisfies the boundary conditions as follows:

$$bc(S(a), S(b)) = 0, \quad (18)$$

and it also satisfies the following differential equations at both ends and mid-point of each subinterval:

$$S'(x_n) = f(x_n, S(x_n)). \quad (19)$$

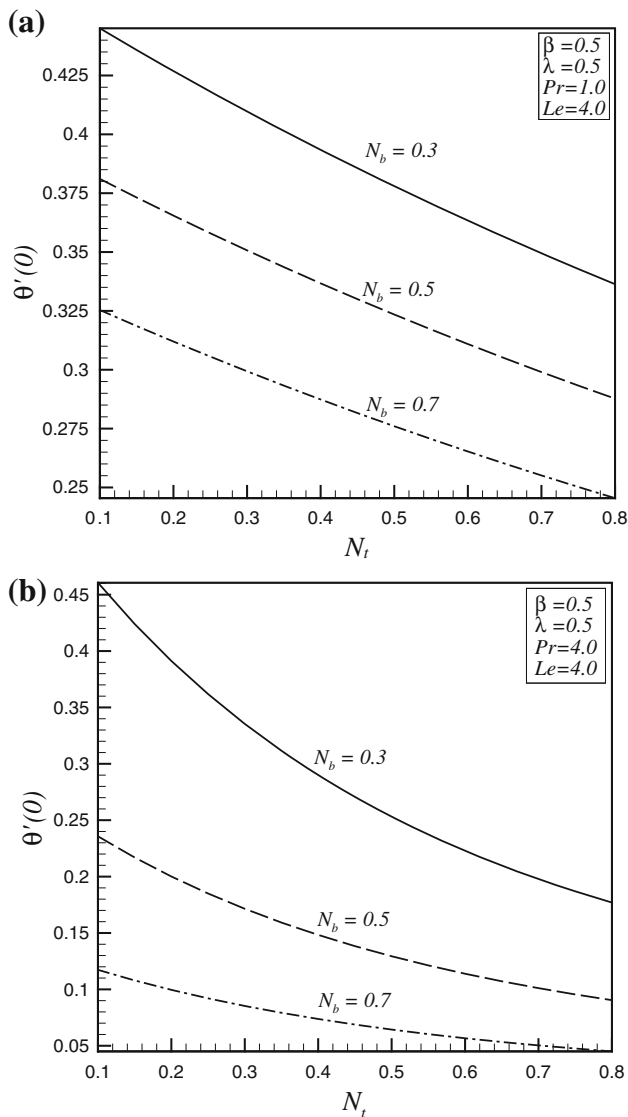


**Fig. 4** Effects of  $N_b$  and  $Pr$  on reduced Nusselt number

$$S'((x_n + x_{n+1})/2) = f((x_n + x_{n+1})/2, S((x_n + x_{n+1})/2)). \quad (20)$$

$$S'(x_{n+1}) = f(x_{n+1}, S(x_{n+1})). \quad (21)$$

These conditions result in a system of nonlinear algebraic equations for the coefficients defining  $S(x)$ , which are solved iteratively by linearization. Here  $S(x)$  is a fourth-order approximation to an isolated solution  $y(x)$ , i.e.,  $\|y(x) - S(x)\| \leq Ch^4$ , where  $h$  is the maximum of the step sizes  $h_n = x_{n+1} - x_n$  and  $C$  is a constant. For such an approximation, the residual  $r(x)$  in the ODEs is defined by

$$r(x) = S'(x) - f(x, S(x)). \quad (22)$$

Mesh selection and error control are based on the residual of the continuous solution. The relative error

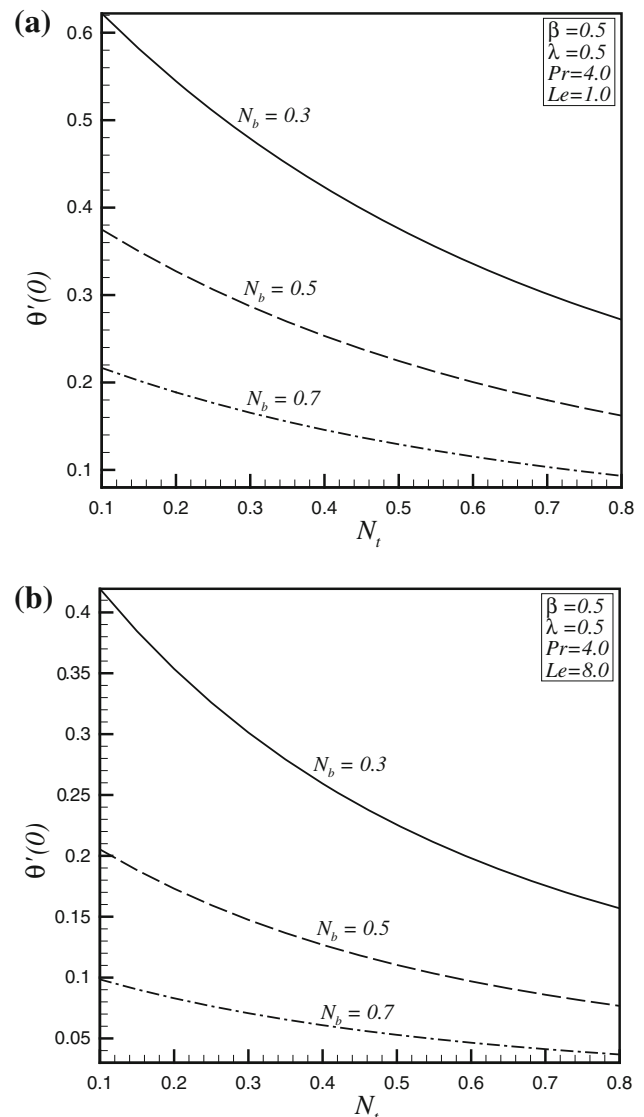


**Fig. 5** Effects of  $N_b$  and  $Le$  on reduced Nusselt number

tolerance was set to  $10^{-10}$ . In this method, we have chosen a suitable finite value of  $\eta \rightarrow \infty$ , namely  $\eta_\infty = \eta_{\max} = 10$ .

## Results and discussions

In the present section, we discussed the emerging parameters such as Deborah number  $\beta$ , ratio of relaxation to retardation times parameter  $\lambda$ , Prandtl parameter  $Pr$ , Brownian parameter  $N_b$ , thermophoresis parameter  $N_t$  and Lewis number  $Le$  for velocity profile  $f'(\eta)$ , temperature profile  $\theta(\eta)$  and nanoparticles fraction  $\phi(\eta)$ . Figure 1a depicts the behavior of  $\beta$  on velocity profile, temperature profile and nanoparticles fraction. It is seen from Fig. 1a that for higher values of Deborah number  $\beta$  velocity

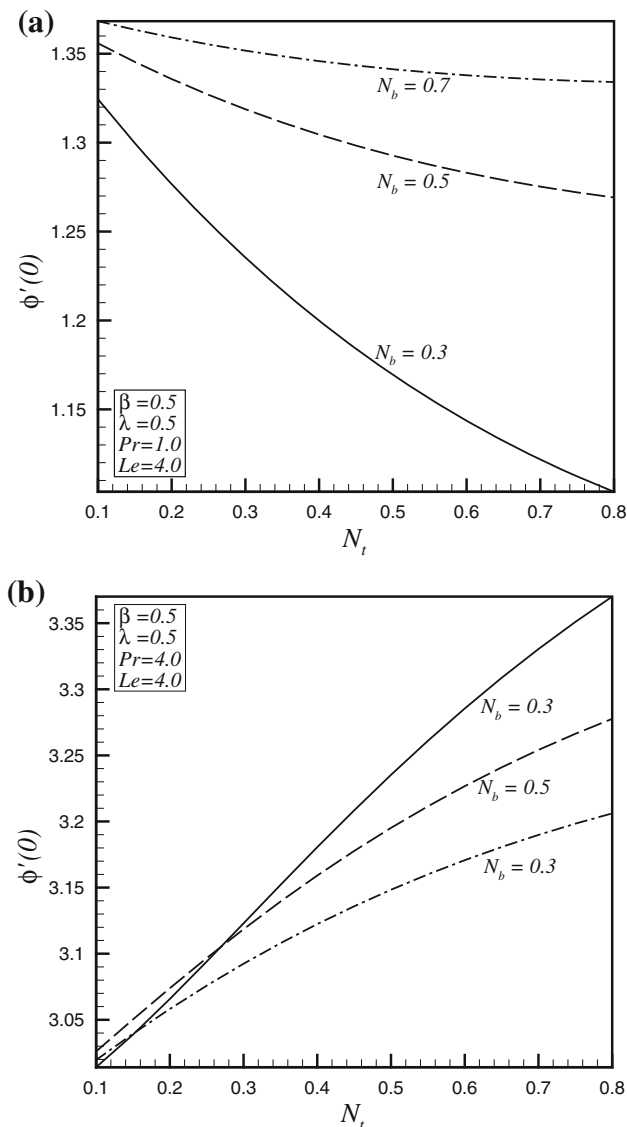


**Fig. 6** Effects of  $N_b$  and  $Pr$  on reduced Sherwood number

increases, while the boundary layer thickness decreases. On the other hand, with an increase of  $\beta$ , both temperature and nanoparticles fractions profile reduces. From Fig. 1b, the effects of  $\lambda$  on velocity, temperature and nanoparticles fraction show opposite behavior when compared with that in Fig. 1a. It is postulated that the increase in elastic parameter will increase the resistance of fluid motion. So in the absence of non-Newtonian effects the present model reduces to the Newtonian model for nanofluid, which present excellent agreement of Khan and Pop (2010). In Fig. 2a and b, we discussed the behavior of both temperature profile  $\theta(\eta)$  and nanoparticles fraction  $\varphi(\eta)$  for two main parameters of nanoparticles Brownian motion  $N_b$  and thermophoresis parameter  $N_t$ . Hypothetically, enhanced thermal conductivity of a nanofluid is mainly due to Brownian motion which produces micro-mixing. As

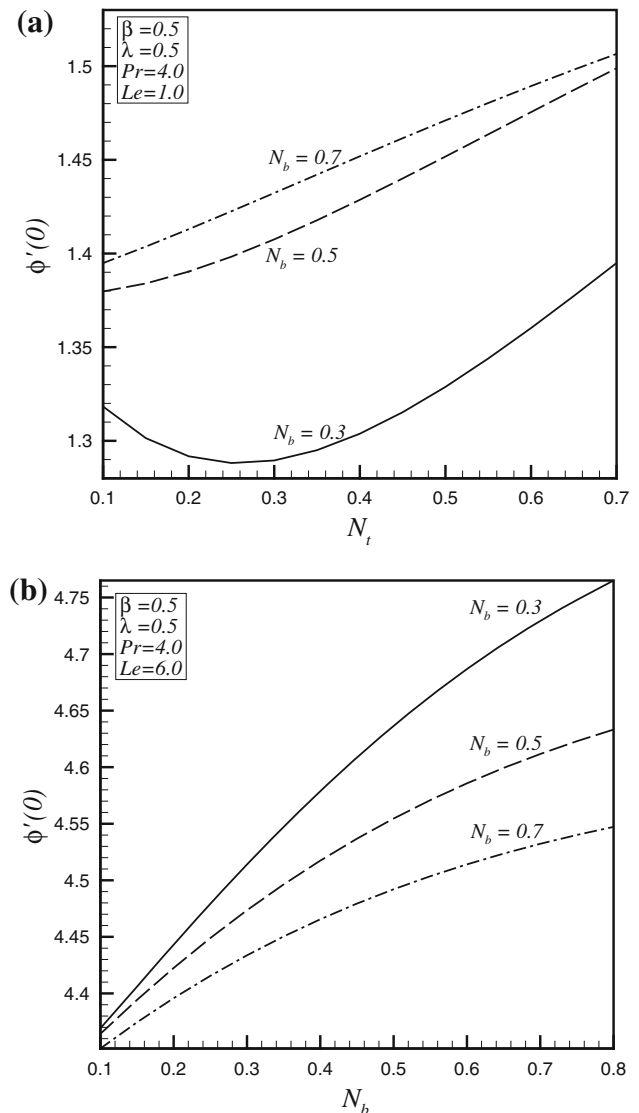


**Fig. 7** Effects of  $N_b$  and  $Le$  on reduced Sherwood number

expected temperature is an increasing function of Brownian parameter (see Fig. 2a). Whereas, large values of Brownian parameter it reduced the nanoparticles fractions. On the other hand, it is observed from Fig. 2b for higher values of thermophoresis parameter  $N_t$  that both temperature and nanoparticles fraction are increasing. Comparatively, it is examined from Fig. 2a and b, that there is an enhancement in temperature with respect to large values of both Brownian and thermophoresis parameter, while opposite behavior can be observed for nanoparticles fraction with the increase of Brownian and thermophoresis parameters (see Fig. 2a, b). The effects of Prandtl number  $Pr$  on  $\theta(\eta)$  and  $\varphi(\eta)$  can be seen in Fig. 3a. Since  $Pr$  is ratio of viscous diffusion rate to the thermal diffusion rate, higher Prandtl number reduces the thermal diffusivity. Consequently, same sort of thing happened with  $Pr$  in



Fig. 3a that for higher values of  $Pr$  it decreases, the both temperature and nanoparticles fractions. It is also illustrated from Fig. 3b that both temperature and nanoparticles fraction shows the opposite behavior for higher values of  $Le$ .

Tables 1 and 2 present the excellent correlation of the mentioned problem with the Khan and Pop (2010) for local Nusselt number  $\theta'(0)$  and Sherwood number  $\phi'(0)$ . It is observed from Tables 1 and 2, in the absence of non-Newtonian effects the present model reduces to the Newtonian model for nanofluid. Table 3 presents the numerical values of both Brownian motion and thermophoresis parameters in the presence of non-Newtonian parameters ( $\beta = \lambda = 0.5$ ), when  $Pr = 10$  and  $Le = 1$ . Effects of physical parameters on non-dimensional Nusselt number  $\theta'(0)$  and Sherwood number  $\phi'(0)$  are also presented through Figs. 4, 5, 6, 7. From Figs. 4 and 5, for increasing values of Brownian motion parameter it reduces the Nusselt number  $\theta'(0)$  for different values of  $Pr$  and  $Le$ . In both the cases, either we take higher values of  $Pr$  (see Fig. 4a, b) or higher values of  $Le$  (see Fig. 5a, b). The same sort of behavior can be seen on reduced Nusselt number  $\theta'(0)$  for higher values of Brownian motion parameter  $N_b$ . From Figs. 6 and 7, Sherwood number  $\phi'(0)$  increases with an increase in Brownian motion parameter  $N_b$ . So it is observed from this phenomena that there is low thermal conductivity for higher Prandtl number.

## Conclusions

In the present study, we have presented the effect of nanoparticles for Jeffrey fluid over a stretching sheet. The effects of elastic parameter, Brownian motion and thermophoresis parameters are also discussed. Numerical solutions for velocity, temperature and nanoparticle fraction are developed and discussed. The main results of present analysis can be listed below.

- Effects of  $\beta$  and  $\lambda$  are opposite for velocity and temperature profile.
- Both  $Pr$  and  $Le$  give same behavior for temperature.
- Effects of  $N_b$  and  $N_t$  for temperature profile are similar
- Effects of  $N_b$  and  $N_t$  for nanoparticle fraction are opposite.
- The magnitude of the local Nusselt numbers decreases for higher values of  $N_b$ .
- The magnitude of the local Sherwood numbers increases for higher values of  $N_b$ .

**Open Access** This article is distributed under the terms of the Creative Commons Attribution License which permits any use,

distribution, and reproduction in any medium, provided the original author(s) and the source are credited.

## References

- Cheng Lixin (2009) Nanofluid heat transfer technologies. *Recent Pat Eng* 3:1–7
- Choi SUS (1995) Enhancing thermal conductivity of fluids with nanoparticles, International Mechanical Engineering Congress and Exposition, San Francisco, USA, ASME, FED 231/MD, vol 66, pp 99–105
- Crane L (1970) Flow past a stretching plate. *Z Angew Math Phys* 21:645–647
- Domairry D, Sheikholeslami M, Ashorynejad HR, Gorla RSR, Khani M (2012) Natural convection flow of a non-Newtonian nanofluid between two vertical flat plates. *J Nanoeng Nanosyst* 225(3):115–122
- Ellahi R (2009) Effects of the slip boundary condition on non-Newtonian flows in a channel. *Commun Nonlinear Sci Numer Simul* 144:1377–1384
- Ellahi R, Afza S (2009) Effects of variable viscosity in a third grade fluid with porous medium: an analytic solution. *Commun Nonlinear Sci Numer Simul* 14(5):2056–2072
- Hamad MAA, Pop I, Md Ismail AI (2011) Magnetic field effects on free convection flow of a nanofluid past a vertical semi-infinite flat plate. *Nonlinear Anal Real World Appl* 12:1338–1346
- Hashim MI, Kandasamy R, Khamis AB (2008) Effect of heat and mass transfer on nonlinear MHD boundary layer flow over a shrinking sheet in the presence of suction. *Appl Math Mech (English Edition)* 29(10):1309–1317
- Khan WA, Aziz A (2011) Double-diffusive natural convective boundary layer flow in a porous medium saturated with a nanofluid over a vertical plate: prescribed surface heat, solute and nanoparticle fluxes. *Int J Therm Sci* 50:2154–2160
- Khan WA, Pop I (2010) Boundary-layer flow of a nanofluid past a stretching sheet. *Int J Heat Mass Transf* 53:2477–2483
- Ma Y, Bhattacharya A, Kuksenok O, Perchak D, Balazs AC (2012) Modeling the transport of nanoparticle-filled binary fluids through micropores. *Langmuir* 28(31):11410–11421
- Nadeem S, Hussain A (2010) HAM solutions for boundary layer flow in the region of the stagnation point towards a stretching sheet. *Commun Nonlinear Sci Numer Simul* 15:475–481
- Nadeem S, Lee C (2012) Boundary layer flow of nanofluid over an exponentially stretching surface. *Nanoscale Res Lett* 7(1): 94
- Nadeem S, Zaheer S, Fang T (2011) Effects of thermal radiation on the boundary layer flow of a Jeffrey fluid over an exponentially stretching surface. *Numer Algorithms* 57:187–205
- Nadeem S, Haq RU, Lee C (2012) MHD flow of a Casson fluid over an exponentially shrinking sheet. *Scientia Iranica* 19(6):1550–1553
- Noor NFM, Awang Kechil S, Hashim I (2010) Simple non-perturbative solution for MHD viscous flow due to a shrinking sheet. *Commun Nonlinear Sci Numer Simul* 15:144–148
- Pearson JRA, Tardy PMJ (2002) Models for flow of non-Newtonian and complex fluids through porous media. *J Non Newton Fluid Mech* 102:447–473
- Sakiadis BC (1961) Boundary-layer behavior on continuous solid surface: I Boundary-layer equations for two-dimensional and axisymmetric flow. *J Am Inst Chem Eng* 7:26–28
- Sebdani SM, Mahmoodi M, Hashemi SM (2012) Effect of nanofluid variable properties on mixed convection in a square cavity. *Int J Heat Mass Transf* 52:112–126
- Xuan Y, Li Q, Hu W (2003) Aggregated structure and thermal conductivity of nanofluids. *AIChE J* 49:1038–1043